Interaction-Driven Spontaneous Quantum Hall Effect on a Kagome Lattice

W. Zhu, Shou-Shu Gong, Tian-Sheng Zeng, Liang Fu, and D. N. Sheng

Phys. Rev. Lett. **117**, 096402 — Published 23 August 2016

DOI: 10.1103/PhysRevLett.117.096402

Interaction-Driven Spontaneous Quantum Hall Effect on Kagome Lattice

W. Zhu[1], Shou-Shu Gong[2], Tian-Sheng Zeng[1], Liang Fu[3] and D. N. Sheng[1]
[1]*Department of Physics and Astronomy, California State University, Northridge, California 91330, USA*
[2]*National High Magnetic Field Laboratory, Florida State University, Tallahassee, Florida 32310, USA and*
[3]*Department of Physics, Massachusetts Institute of Technology, Cambridge, Massachusetts 02139, USA*

Topological states of matter have been widely studied as being driven by external magnetic field, intrinsic spin-orbital coupling or magnetic doping. Here, we unveil an interaction-driven spontaneous quantum Hall effect (Chern insulator) emerging in an extended fermion-Hubbard model on a kagome lattice, based on the state-of-the-art density-matrix renormalization group on cylinder geometry and exact diagonalization on torus geometry. We first demonstrate the proposed model exhibits an incompressible liquid phase with doublet degenerate ground states as time-reversal partners. The explicit time-reversal symmetry spontaneously breaking is determined by emergent uniform circulating loop-currents between nearest neighbors. Importantly, the fingerprint topological nature of ground state is characterized by quantized Hall conductance. Thus, we identify the liquid phase as a quantum Hall phase, which provides a "proof-of-the-principle" demonstration of interaction-driven topological phase in a topologically trivial non-interacting band.

Introduction.— Topological states of matter has led to an ongoing revolution of our fundamental understanding of quantum materials, as exemplified by the discoveries of integer quantum Hall (IQH) effect [1, 2], quantum anomalous Hall (QAH) effect [3–5] and quantum spin Hall effect [6–8]. Crucially, such topological phases emerge from non-interacting electronic structures with nontrivial topology, where a strong magnetic field or a large spin-orbit coupling is typically necessary. Despite great achievements, so far most of the materials that exhibit unique topological properties can be understood based on non-interacting physics originating from nontrivial band physics. This limitation inspires recent enthusiasm in exploring topological phases in "trivial" materials [9–13], without the requirement of a nontrivial invariant encoded in single-particle wavefunction or band structure. Finding such kind of novel phases can significantly enrich the class of topological materials and is thus of great importance.

The strong correlation between electrons can dramatically change the non-interacting physics and induce spontaneous symmetry breakings. Therefore, many-body interaction is expected to enable topological phases in strongly-correlated systems by generating circulating currents and spontaneously breaking time-reversal symmetry (TRS), which act as an effective magnetic field or spin-orbit coupling [12, 14, 15]. This subject has undergone vigorous research due to supports from mean-field studies followed by low-energy renormalization group analysis [13, 16], and then the existence of such topological phases has been suggested for the extended Hubbard model on various lattice models [17–30]. However, unbiased numerical simulations, such as exact diagonalization (ED) and density matrix renormalization group (DMRG) studies, found other competing states rather than topological phases as the true ground states in *all* previously proposed systems with Dirac points [31–34] or quadratic band touching points [35, 36]. A major obstacle is, instead of triggering the desired TRS spontaneously breaking, strong interactions tend to stabilize competing solid orders by breaking translational or rotational lattice symmetry. Thus, the putative topological phase is usually preempted by various competing states [31–36]. Moreover, it is also technically challenging to detect such kind of exotic phases with spontaneously TRS breaking, as the TRS partners usually tend to couple together on finite-size systems. If the intrinsic energy gap generated by TRS breaking is small, numerical simulations can hardly distinguish a possible insulating topological phase from the semimetal phase [34]. Taken as a whole, the simple concept of realizing interaction-induced topological phases remains unsettled for realistic electron systems, and so far what type of physically attainable Hamiltonians would exhibit these exotic ground states has yet to be established.

In this paper, we provide unbiased numerical evidences of a QAH phase generated by electron-electron interactions in a fermion-Hubbard model on kagome lattice. By engineering electron interactions, our ED calculations signal an incompressible liquid phase with a doublet degenerate ground states on torus geometry. To further investigate the nature of this gapped phase, we perform DMRG calculation on cylinder geometry for larger systems. Remarkably, we show the TRS of ground state is spontaneously TRS breaking, with the compelling evidence from emergent long-ranged and uniform circulating loop-currents. The topological nature of the ground state is identified by quantized Hall conductance, with the help of the idea similar to Laughlin gedenkan experiment performed numerically. Thus we establish that the essence of the gapped phase is equivalent to the QAH phase. We also confirm the QAH phase is robust against finite-size effects, by accessing large systems up to the current computational limit. Moreover, we map out a phase diagram and identify two competing charge density wave phases by varying interactions, where transitions to the QAH phase are determined to be of the first order. Our results not only provide "fingerprint" evidences of the interaction-driven QAH phase, but also open up a long-sought platform for exploring topological physics in strongly-correlated systems.

Model and Method.— We consider a spinless fermion-Hubbard model on a kagome lattice shown in the inset of Fig.

1(a) and described by the Hamiltonian:

$$H = t\sum_{\langle \mathbf{r}\mathbf{r}'\rangle}\left[c^{\dagger}_{\mathbf{r}'}c_{\mathbf{r}} + \text{H.c.}\right] + V_1\sum_{\langle \mathbf{r}\mathbf{r}'\rangle} n_{\mathbf{r}}n_{\mathbf{r}'} + V_2\sum_{\langle\langle \mathbf{r}\mathbf{r}'\rangle\rangle} n_{\mathbf{r}}n_{\mathbf{r}'} + V_3\sum_{\langle\langle\langle \mathbf{r}\mathbf{r}'\rangle\rangle\rangle} n_{\mathbf{r}}n_{\mathbf{r}'}, \quad (1)$$

where $c^{\dagger}_{\mathbf{r}}$ ($c_{\mathbf{r}}$) creates (annihilates) a spinless fermion at site $\mathbf{r}$. We set the nearest-neighbor hopping amplitude $t = 1$ as energy unit here. V_1, V_2, V_3 denote the density-density repulsion strengths on first, second and third nearest neighbors, respectively [38]. We focus on the total filling number $\nu = N_e/N_s = 1/3$ (N_e is the total electron number and N_s is the number of the lattice sites). In the non-interacting limit, this model supports three energy bands and the lowest flat band quadratically touches the second band at the Γ point ($K = (0, 0)$) [37], thus the system is gapless at $\nu = 1/3$ and topological trivial.

In order to study the ground state phase diagram in the $\{V_1, V_2, V_3\}$ parameter space, we implement the DMRG algorithm [39, 40] combined with ED, both of which have been proven to be powerful and complementary tools for studying realistic models containing arbitrary strong and frustrated interactions [41–47]. We study large systems up to $L_y = 6$ unit cells and keep up to $M = 4800$ states to guarantee a good convergence (the discarded truncation error is less than 2×10^{-6}). We take advantage of the recent development in DMRG algorithm by adiabatically inserting flux to probe the TRS spontaneous breaking and the topological quantized Hall conductance (see [37] for computational details) [43–46].

Phase diagram.— In the presence of strong interactions, our main findings are summarized in the phase diagram Fig. 1(a-b). In the intermediate parameter region (labeled by red), we find a robust QAH phase emerging with the TRS spontaneously breaking. The QAH phase is featured by a twofold ground state degeneracy on torus geometry, arising from two sets of QAH states with opposite chiralities. The topological nature of the QAH states are characterized by the integer quantized Chern numbered $C = \pm 1$ for the TRS breaking states with the opposite chiralities, respectively. In addition, we also show that the QAH phase is neighboring with several solid phases which all respect TRS: a stripe phase and a charge density wave phase, both demonstrating distinctive Bragg peaks in their density-density structure factors (Fig. 1(c-d)). On the contrary, the QAH phase displays a structureless feature (Fig. 1(e)) in the structure factor, indicating the absence of the space-group symmetry breaking. Finally, reducing V_1, V_2 and V_3 simultaneously, we find a parameter region shaded by light red in the left bottom corner in the phase diagram Fig. 1(a-b), which is likely a weaker QAH phase (labeled as QAH*) as we discuss more details later.

Energy Spectrum and Double Degeneracy.— The emergent QAH phase on a finite torus system is expected to host a twofold ground state degeneracy, representing two TRS spontaneously breaking states with the opposite chiralities as TRS partners to each other. To examine this property for the model

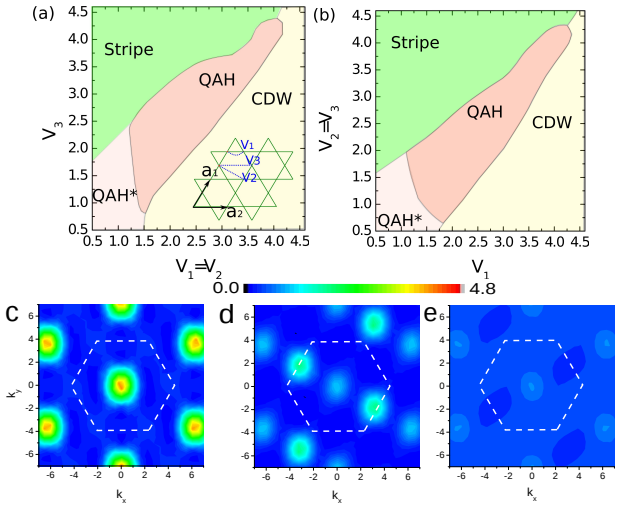

FIG. 1: Phase diagram of an extended fermion Hubbard model (Eq. 1) plotted in (a) $V_1 = V_2$ and V_3 parameter space and in (b) V_1 and $V_2 = V_3$ parameter space, obtained by DMRG calculations on cylinder of circumference $L_y = 6$. The QAH phase is characterized by the long-ranged current-current correlations and integerly quantized Hall conductance. The phase boundary between QAH phase and other phase is determined by the emergent loop current which signals TRS spontaneously breaking. The contour plots of static density structure factor for: (c) charge density wave $q = (0, 0)$ phase, (d) stripe phase and (e) QAH phase. The white dashed line shows the first Brillouin zone.

systems, we first investigate the low-energy spectra based on ED calculation. As shown in Fig. 2 (a), we find two near degenerating ground states in energy spectra for both $N_s = 27$ and 36 clusters [51], which are separated from the excited levels by a finite energy gap. Importantly, the ground states never mix with excited levels with varying the twisting boundary conditions, signaling the robustness of excitation gap (see [37]). Moreover, a stable topological phase is expected to be protected, not only by excitation gap, but also by nonzero single-particle gap. In Fig. 2(b), we also calculated the single-particle gap $\Delta(N_s)$ as a function of $1/N_s$, where the finite-size scalings indicate a nonzero $\Delta(\infty)$ for QAH phase.

Time Reversal Symmetry Spontaneously Breaking and Emergent Loop Current.— To investigate the possible TRS *spontaneously* breaking of the ground states, we turn to larger systems on the cylinder geometry and obtain the ground states by implementing DMRG calculation. Indeed, we obtain two TRS breaking states $|\Psi^{L(R)}\rangle$ by random initializations of wavefunctions in DMRG simulations [41], which are degenerating in energy as expected (as the TRS partner to each other). Here we label different groundstates by their chiral nature, where L (R) stands for "left-hand" ("right-hand") chirality. The corresponding TRS spontaneously breaking of $|\Psi^{L(R)}\rangle$ can be obtained by measuring emergent currents $\mathcal{J}_{ij} = i\langle\Psi^{L(R)}|c^{\dagger}_i c_j - c^{\dagger}_j c_i|\Psi^{L(R)}\rangle$ between two nearest-neighbor sites (i, j). As shown in Fig. 3 (a), local current pattern $\mathcal{J}_{ij}$ uniformly distributes (arrow representing direction of current), which excludes the possibility of bond modulated

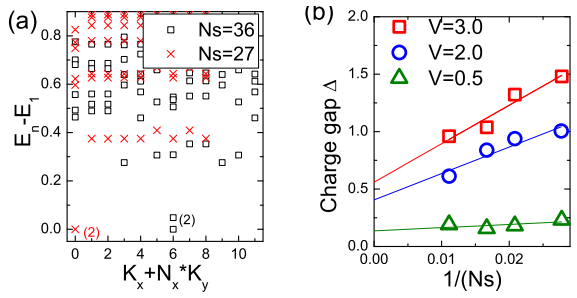

FIG. 2: (a) Energy spectra from ED versus momentum quantum numbers (K_x, K_y) on the $N_s = 3 \times 3 \times 3 = 27$ (red cross) and $N_s = 3 \times 3 \times 4 = 36$ (black square) sites cluster, by setting $V = V_1 = V_2 = V_3$ and $V = 3.95$. The ground state degeneracy are labeled by numbers. (b) Finite-size extrapolations of single-particle gap $\Delta(N_s) = E(N_s, N_e - 1) + E(N_s, N_e + 1) - 2E(N_s, N_e)$ obtained by DMRG ($E(N_s, N_e)$ the ground state energy on $N_s = 3 \times N_x \times N_y$ with N_e electrons) on several lattice clusters: $3 \times 3 \times 4$, $3 \times 4 \times 4$, $3 \times 4 \times 5$, $3 \times 5 \times 6$.

local orders. Most importantly, local currents pattern form loop structure circulating in the anti-clockwise direction in each hexagon for $|\Psi^L\rangle$ (We have checked that the TRS partner $|\Psi^R\rangle$ hosts clockwise loop current). Interestingly, the staggered magnetic flux in each unit cell (enclosing one hexagon and two triangular) averages out to zero, exactly matching the expectation of constructed model for QAH effect [3, 16].

Moreover, we also calculate the current-current correlation functions $\langle \mathcal{J}_{ij} \mathcal{J}_{i_0 j_0} \rangle$ in Fig. 3(b) ((ij) is the bond parallel with the reference bond $(i_0 j_0)$ and the distance measured by R_{ij}). We compare $\langle \mathcal{J}_{ij} \mathcal{J}_{i_0 j_0} \rangle$ for QAH phase with different system widths. We find long-range correlations for all system

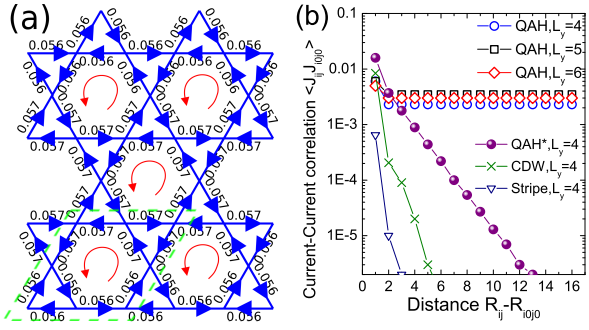

FIG. 3: (a) Real-space plot of emergent current pattern $\mathcal{J}_{ij}$ (we only show a section of three columns on $L_y = 4$ cylinder), for $|\Psi^L\rangle$ with left chirality. The width of the bond is proportional to the absolute value (shown on the bond as a number) and arrows point to current directions. The red arrow indicates the current direction in each hexagon. (b) Log-linear plot of current-current correlations $\langle \mathcal{J}_{ij} \mathcal{J}_{i_0 j_0} \rangle$ versus distance $R_{ij} - R_{i_0 j_0}$ for QAH phase with system width $L_y = 4$ (blue square), $L_y = 5$ (black square) and $L_y = 6$ (red square). All correlations demonstrate long-range order (and they are also positive) for the QAH phase, while $\langle \mathcal{J}_{ij} \mathcal{J}_{i_0 j_0} \rangle$ decay exponentially in stripe phase and charge density wave phase. The real-space plot of current-current correlations is shown in Ref. [37].

widths $L_y = 4, 5, 6$. The current correlations keep stable with increasing L_y, indicating the TRS spontaneously breaking is robust against finite-size effects. In contrast, the current correlations decay exponentially for stripe phase and charge density wave phase, revealing the TRS preserving in solid phases. As last, we notice that QAH* phase can develop a relatively weaker current correlation, albeit it shows sharply decaying correlation in short-range distance.

Quantized Hall conductance.— To uncover the topological nature of the QAH phase, we perform a numerical flux insertion simulation on cylinder system [43, 47] to determine the quantized Hall conductance σ_H. This simulation follows the idea of Laughlin gedanken experiment for interpreting IQH effect [2, 52], where an integer quantized charge will be pumped from one edge to the other edge by inserting a $U(1)$ charge flux θ in the hole of the cylinder. At the DMRG side, we adiabatically increase the inserted flux θ and use the converged wavefunction for smaller θ as the initial state for the increased θ to achieve adiabatical evolution of the ground state [37, 43]. The Hall conductance can be computed by $\sigma_H = \frac{e^2}{h} \Delta Q|_{\theta=0}^{\theta=2\pi}$ [43, 47], where the net charge transfer $\Delta Q(\theta)$ can be calculated from the net change of the total charge in the half system: $\Delta Q(\theta) = Tr[\hat{\rho}_L(\theta)\hat{Q}]$ ($\hat{\rho}_L$ the reduced density matrix of left half cylinder). As expected, in Fig. 4(a), the obtained σ_H of QAH phase takes nearly quantized value $\sigma_H \approx -1.00 e^2/h$ (for $|\Psi^L\rangle$) by threading a flux quantum $\theta = 0 \to 2\pi$. We also checked that the TRS partner $|\Psi^R\rangle$ hosts $\sigma_H \approx 1.00 \frac{e^2}{h}$. In comparison, both the stripe phase and charge density wave do not respond to the inserted flux, therefore have exactly zero Hall conductance $\sigma_H = 0$ (Fig. 4(a)) consistent with the trivial topology of these states. Furthermore, we examine the stability of the topological quantization on finite-size systems. In Fig. 4(b), we show the Hall conductance σ_H of the QAH phase on cylinder system with widths $L_y = 4, 5, 6$, all of which give nearly quantized value $\sigma_H \approx -1.00 \frac{e^2}{h}$, supporting that the QAH phase is stable in the thermodynamic limit.

Phase transition.— We address the nature of the quantum phase transitions between the QAH phase and other phases (see [37]). We utilize several quantities, such as groundstate wavefunction fidelity, which are expected to signal the sensitivity of the wavefunction with varying interacting parameters. Moreover, we have also inspected several order parameters related to TRS and translational symmetry spontaneously breakings[37], respectively. Based on these studies, we find that transitions between the QAH phase and the stripe phase as well as charge density wave phase are the first order ones, with evidences from step-like change in wavefunction overlap and order parameters [37].

Even though the QAH phase is shown to be remarkably robust in the phase diagram, we are less certain about the QAH* phase (sitting at the left bottom corner of Fig. 1). We do not observe TRS breaking (or long-ranged current correlations) in QAH* phase (Fig. 3(b)). Interestingly, if we perform flux insertion (inducing TRS breaking explicitly), we observe

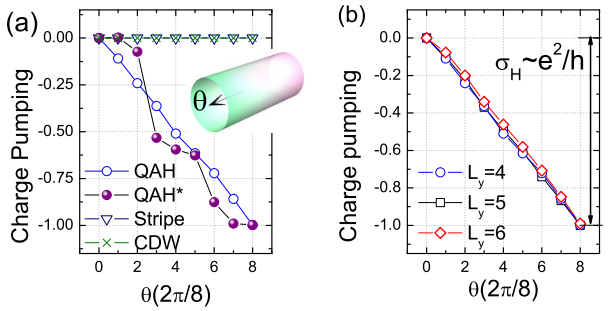

FIG. 4: Hall conductance σ_H obtained by Laughlin flux insertion gedanken experiment, where σ_H equals to the charge transfer ΔQ from one edge to the other edge. (a) Net charge transfer ΔQ for QAH phase (blue circle), stripe phase (navy triangular), charge density wave (green cross) and QAH* phase (purple dot). The system size is $L_y = 4$ cylinder. Inset cartoon illustrates adiabatically threading a $U(1)$ charge flux in the hole of cylinder. (b) Net charge transfer ΔQ of QAH phase for different system sizes $L_y = 4$ (blue circle), $L_y = 5$ (black square) and $L_y = 6$ (red diamond).

a nearly quantized Hall conductance (Fig. 4(a)), while the evolution of the pumped charge versus flux is not as smooth as the QAH phase. Hence, we believe that the ground state of the QAH* phase is a QAH state, however with strong finite size effect (as indicated by relatively small energy gap in Fig. 2(b)). In addition, going closer to the weak interaction limit, using ED calculations, we find the ground state remains to evolve adiabatically from QAH phase to QAH* phase without additional quantum phase transition [37], which is consistent with the mean-field[16, 37] and perturbative renormalization-group[25] prediction of infinitesimal interaction inducing QAH effect.

Conclusion and Outlook.— We have presented convincing evidences of an interaction-driven spontaneous quantum anomalous Hall (QAH) phase in an extended Fermion-Hubbard model on kagome lattice at one-third filling through engineering interactions. Our complete characterization of the universal properties of the QAH phase includes ground state degeneracy, time-reversal symmetry (TRS) spontaneously breaking, and the quantized Hall conductance, all of which provide an unambiguous diagnose of a QAH phase. Such an exotic state had been sought after for a long time, however, its existence in a microscopic model has remained elusive until now. Our current results offer a "proof-of-the-principle" demonstration of the spontaneous QAH purely driven by interactions, without the need of external magnetic field or other mechanism of explicit TRS breaking. We believe our work will stimulate future research along a number of directions. For example, introducing additional degrees of freedom in simple models usually results in richer behaviors, hence our current model with including spin or orbital degrees will provide a promising playground for synthesising and engineering other exotic states, such as an emergent quantum spin Hall effect [6–8, 53] without spin-orbital coupling. Moreover, the lowest energy band on kagome lattice is exactly flat [37, 48–50], thus one could imagine a nearly flat band with non-zero Chern number after the gap opening by interactions. This would be quite significant since it may provide a platform to realize the spontaneously fractional QAH phase or fractional Chern insulators [54–61] when such flat band is partially filled. At experimental side, based on the recently experimental development of artificial kagome systems [62], we anticipate activities to realize and detect the QAH state in ultracold atomic systems [63].

Acknowledgements.— We thank K. Sun and Y. Zhang for stimulating discussions. This research is supported by the DOE office of Basic Energy Sciences under grants No. DE-FG02-06ER46305 (W.Z., D.N.S). S.S.G is supported by the National High Magnetic Field Laboratory (NSF DMR-1157490) and the State of Florida. L.F. is supported by the DOE office of Basic Energy Sciences, Division of Materials Sciences and Engineering under award DE-SC0010526. We also acknowledge partial support from NSF grant DMR-1532249 for computational resource.

Note added. During the final stages of the completion of this manuscript, we became aware of a work claiming a QAH phase on a checkerboard lattice based on ED calculation on small sizes [64] (see also [65]).

[1] K. v. Klitzing, G. Dorda, and M. Pepper, Phys. Rev. Lett. **45**, 494 (1980).
[2] R. B. Laughlin, Phys. Rev. B **23**, 5632 (1981).
[3] F. D. M. Haldane, Phys. Rev. Lett. **61**, 2015 (1988).
[4] C.-Z. Chang, J. Zhang, X. Feng, J. Shen, Z. Zhang, M. Guo, K. Li, Y. Ou, P. Wei, L. Wang, et al., Science **340**, 167 (2013).
[5] C. X. Liu, S. C. Zhang and X. L. Qi, Annu. Rev. Condens. Matter Phys. **7**, 301-321 (2016).
[6] C. L. Kane and E. J. Mele, Phys. Rev. Lett. **95**, 226801 (2005).
[7] X. L. Qi and S. C. Zhang, Rev. Mod. Phys. **83**, 1057 (2011).
[8] M. Z. Hasan and C. L. Kane, Rev. Mod. Phys. **82**, 3045 (2010).
[9] N. H. Lindner, G. Refael, and V. Galitski, Nat. Phys. **7**, 490 (2011).
[10] T. Kitagawa, T. Oka, A. Brataas, L. Fu, and E. Demler, Phys. Rev. B **84**, 235108 (2011).
[11] S. Diehl, E. Rico, M. A. Baranov, and P. Zoller, Nat. Phys. **7**, 971-977 (2011).
[12] C. Wu and S.-C. Zhang, Phys. Rev. Lett. **93**, 036403 (2004).
[13] S. Raghu, X.-L. Qi, C. Honerkamp, and S.-C. Zhang, Phys. Rev. Lett. **100**, 156401 (2008).
[14] X. G. Wen, F. Wilczek, and A. Zee, Phys. Rev. B **39**, 11413 (1989).
[15] X. G. Wen, Phys. Rev. B **44**, 2664 (1991).
[16] K. Sun, H. Yao, E. Fradkin, and S. A. Kivelson, Phys. Rev. Lett. **103**, 046811 (2009).
[17] J. Wen, A. Rüegg, C.-C. J. Wang, and G. A. Fiete, Phys. Rev. B **82**, 075125 (2010).
[18] Y. Zhang, Y. Ran, and A. Vishwanath, Phys. Rev. B **79**, 245331 (2009).
[19] M. Kurita, Y. Yamaji, and M. Imada, Journal of the Physical Society of Japan p. 044708 (2011).
[20] C. Weeks and M. Franz, Phys. Rev. B **81**, 085105 (2010).
[21] A. Rüegg and G. A. Fiete, Phys. Rev. B **84**, 201103 (2011).
[22] K.-Y. Yang, W. Zhu, D. Xiao, S. Okamoto, Z. Wang, and

Y. Ran, Phys. Rev. B **84**, 201104 (2011).
[23] S. Kitamura, N. Tsuji, and H. Aoki, Phys. Rev. Lett. **115**, 045304 (2015).
[24] S. Uebelacker and C. Honerkamp, Phys. Rev. B **84**, 205122 (2011).
[25] J. M. Murray and O. Vafek, Phys. Rev. B **89**, 201110 (2014).
[26] W.-F. Tsai, C. Fang, H. Yao, and J.-P. Hu, New J. Phys. **17**, 055016 (2015).
[27] A. Dauphin, M. Mller, and M. A. Martin-Delgado, Phys. Rev. A **93**, 043611 (2016).
[28] B. Dóra, I. F. Herbut, and R. Moessner, Phys. Rev. B **90**, 045310 (2014).
[29] R. Nandkishore and L. Levitov, Phys. Rev. B **82**, 115124 (2010).
[30] S. Pujari, T. C. Lang, G. Murthy, R. K. Kaul, arXiv.1604.03876.
[31] N. A. García-Martínez, A. G. Grushin, T. Neupert, B. Valenzuela, and E. V. Castro, Phys. Rev. B **88**, 245123 (2013).
[32] M. Daghofer and M. Hohenadler, Phys. Rev. B **89**, 035103 (2014).
[33] J. Motruk, A. G. Grushin, F. de Juan, and F. Pollmann, Phys. Rev. B **92**, 085147 (2015).
[34] S. Capponi and A. M. Läuchli, Phys. Rev. B **92**, 085146 (2015).
[35] S. Nishimoto, M. Nakamura, A. O'Brien, and P. Fulde, Phys. Rev. Lett. **104**, 196401 (2010).
[36] F. Pollmann, K. Roychowdhury, C. Hotta, and K. Penc, Phys. Rev. B **90**, 035118 (2014).
[37] See Supplemental Material, which includes Refs. [2, 39–50], for a introduction of computational method, a detailed analysis of Kagome band structure in non-interacting limit, a real-space plot of current-current correlation of QAH phase, the evolution of order parameters when crossing the phase boundary, and the mean-field analysis of Hamiltonian.
[38] For the same model with only considering the V_1 interaction, earlier DMRG simulations did not find any TRS breaking states [35].
[39] S. R. White, Phys. Rev. Lett. **69**, 2863 (1992).
[40] I. P. McCulloch, ArXiv e-prints (2008), 0804.2509.
[41] L. Cincio and G. Vidal, Phys. Rev. Lett. **110**, 067208 (2013).
[42] H. C. Jiang, Z. Wang, and L. Balents, Nat. Phys. **8**, 902 (2012).
[43] S. S. Gong, W. Zhu, and D. N. Sheng, Sci. Rep. **4**, 06317 (2014).
[44] Y.-C. He, D. N. Sheng, and Y. Chen, Phys. Rev. B **89**, 075110 (2014).
[45] A. G. Grushin, J. Motruk, M. P. Zaletel, and F. Pollmann, Phys. Rev. B **91**, 035136 (2015).
[46] W. Zhu, S. S. Gong, F. D. M. Haldane, and D. N. Sheng, Phys. Rev. B **92**, 165106 (2015).
[47] M. P. Zaletel, R. Mong, and F. Pollmann, J. Stat. Mech. p. P10007 (2014).
[48] C. Wu, D. Bergman, L. Balents, and S. Das Sarma, Phys. Rev. Lett. **99**, 070401 (2007).
[49] D. L. Bergman, C. Wu, and L. Balents, Phys. Rev. B **78**, 125104 (2008).
[50] J. Schulenburg, A. Honecker, J. Schnack, J. Richter, and H.-J. Schmidt, Phys. Rev. Lett. **88**, 167207 (2002).
[51] For $N_s = 3 \times 3 \times 3 = 27$ cluster, the lowest states are exactly degenerating protected by the rotational symmetry. Nevertheless, due to the finite-size effect, on system $N_s = 36$ there is a finite splitting between lowest two states.
[52] D. N. Sheng, X. Wan, E. H. Rezayi, K. Yang, R. N. Bhatt, and F. D. M. Haldane, Phys. Rev. Lett. **90**, 256802 (2003).
[53] D. N. Sheng, Z. Y. Weng, L. Sheng, and F. D. M. Haldane, Phys. Rev. Lett. **97**, 036808 (2006).
[54] E. Tang, J.-W. Mei, and X.-G. Wen, Phys. Rev. Lett. **106**, 236802 (2011).
[55] T. Neupert, L. Santos, C. Chamon, and C. Mudry, Phys. Rev. Lett. **106**, 236804 (2011).
[56] K. Sun, Z. Gu, H. Katsura, and S. Das Sarma, Phys. Rev. Lett. **106**, 236803 (2011).
[57] D. Sheng, Z.-C. Gu, K. Sun, and L. Sheng, Nat Commun **2**, 389 (2011).
[58] E. J. Bergholtz, and Z. Liu, Int. J. Mod. Phys. B **27**, 1330017 (2013).
[59] S. H. Simon, F. Harper, and N. Read, Phys. Rev. B **92**, 195104 (2015).
[60] We emphasize that our study is distinct from previously proposed Chern insulators or fractional Chern insulators [54–58], where non-trivial band structures in non-interacting limit play a vital role in stabilizing the topological phases. In current model (Eq. 1), non-interacting band structure is trivial (see Ref. [37]), and resulting topological nature of ground states completely comes from the strong correlations.
[61] W. Zhu, S. S. Gong, and D. N. Sheng, Phys. Rev. B **94**, 035129 (2016).
[62] G.-B. Jo, J. Guzman, C. K. Thomas, P. Hosur, A. Vishwanath, and Dan M. Stamper-Kurn, Phys. Rev. Lett. **108**, 045305 (2012).
[63] G. Jotzu, M. Messer, R. Desbuquois, M. Lehrat, T.Uehlinger, D. Greif, and T. Esslinger, Nature **515**, 237-240 (2014).
[64] H. Q. Wu, and Y. Y. He, and C. Fang, and Z. Y. Meng, and Z. Y. Lu, arXiv.1602.02034.
[65] The twofold groundstate degeneracy is not robust against twisted boundary condition, as shown in Fig. S3 ([64]), indicating excitation gap is actually vanishing in finite-size calculations on cherkerboard lattice.